International Journal of Research and Review
Volume 11; Issue: 9; September 2024
Website: www.ijrrjournal.com
Research Paper *E-ISSN: 2349-9788; P-ISSN: 2454-2237*

Study of the Behaviour of a Pile Under Axial Load by Comparative Analysis of Different Models of the *t-z* and *q-z* Load Transfer Curve Method

Cheikh Ibrahima Tine[1], Oustasse Abdoulaye Sall[1], Déthié SARR[2]

[1]Department of Civil Engineering, UFR SI-University Iba Der THIAM of Thiès, Thiès, Senegal
[2]Department of Geotechnics, UFR SI-University Iba Der THIAM of Thiès, Thiès, Senegal

Corresponding Author: Cheikh Ibrahima Tine

DOI: https://doi.org/10.52403/ijrr.20240903

ABSTRACT

This article deals with the determination of axial deformations and axial forces, taking into account the complex interaction between the pile and the surrounding soil. The load transfer curve method, which offers an analytical approach to calculating deformations and axial forces along the pile, is the one used in this study. This method relies on the progressive mobilization of lateral friction and tip pressure, modeled by ***t-z*** (lateral friction) and ***q-z*** (tip pressure) curves, to simulate soil-pile interactions. Several behavioral models based on this method are examined, including linear, trilinear, hyperbolic and exponential laws. Each of these models is analyzed for its ability to predict pile settlement and axial forces, as a function of specific soil and pile characteristics. Frank and Zhao's model, based on the results of the pressuremeter test, proved particularly effective. The results highlight the effectiveness of the load transfer curve method, and underline the importance of choosing the right behavior model for better settlement prediction and design of these foundations.

Keywords: Pile behavior, Axial loads, Settlement, Soil-pile interaction, Load transfer curve method, Lateral friction, Peak pressure.

I. - INTRODUCTION

Before the advent of in-situ testing, the classical theory of load-bearing capacity was used to determine the ultimate load from the mechanical characteristics ***c*** and ***φ***. Classical bearing capacity theory does not take into account pre-failure soil deformation or compressibility, although recent research has highlighted their influence. Furthermore, the literature on piles proposes various approaches to the mechanism of soil failure, complicating the choice of bearing capacity factor formulas. Finally, experience shows that methods based on laboratory tests (***c*** and ***φ***) often poorly predict the results obtained from static pile loading tests (Bouafia, 2018). It should also be pointed out that in the literature, several behavior laws for axially loaded piles are based on the transfer curve method. The first of these curves was proposed by Coyle and Reese in 1966. This study is based on the use of this method to predict displacements under axial load. The ***t-z*** method has been widely used for estimating pile displacement under axial loading, and its results are considered satisfactory (Frank and Zhao, 1982; Maleki, 1995). Generally, the various laws proposed by different authors are classified into five categories: linear (Randolph and Wroth (1978), Verbrugge (1981)), trilinear (Frank and Zhao (1982)), root function (Krasinski (2012), Vijayvergiya (1977)), hyperbolic (Hirayama (1992), Fleming (1992)),

exponential (Wang et al., (2012) and Combarieu (1988), Abchir and Burlon (2016)). In the following, we propose to make a comparative study of the behavior of a pile under axial load in a homogeneous clay soil layer according to the following behavior laws:

- Verbrugge's linear law
- Frank and Zhao's trilinear law
- Hirayama's hyperbolic law of
- Abchir and Burlon's AB1 exponential law

These choices are based on the fact that these laws follow a different distribution, with soil parameters established differently (pressiometric or penetrometric tests), that they are adapted to fine soils and that their reliability has been tested on the basis of pile loading tests. In this work, we propose to study the response of a pile under axial load, by comparative analysis of different models of *t-z* and *q-z* load transfer curves.

II. - METHODS FOR CALCULATING THE VERTICAL BEARING CAPACITY OF AN ISOLATED PILE

The vertical loading of a pile results in the mobilization of a vertical pressure $\boldsymbol{q_p}$ and shear stresses $\boldsymbol{\tau(z)}$ along the pile shaft (Figure 1).

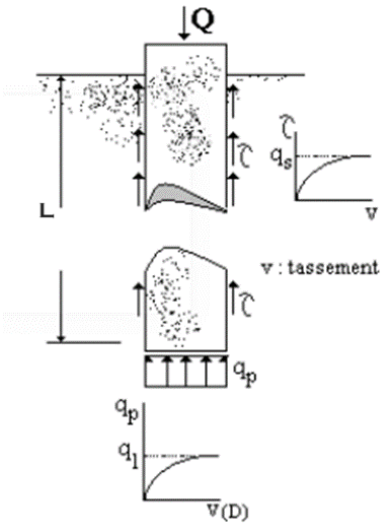

Figure 1. - Pile equilibrium diagram under vertical load (Bouafia, 2018)

As the applied load $\boldsymbol{Q}$ increases, the balance of forces results in a simultaneous increase in the lateral friction stress $\boldsymbol{\tau(z)}$ along the shaft and in the pile tip pressure q_p:

$$Q = A_p q_p + P \int_0^L \tau(z) dz \qquad [1]$$

P and A_p are respectively the perimeter of the shaft and the cross-sectional area of the pile tip.

Several methods are used to calculate pile bearing capacity. Dimensioning methods based on in situ tests are widely used and are currently enjoying considerable growth worldwide. These methods take account of soil heterogeneity by using the concept of equivalent homogeneous soil, characterized by an equivalent resistance named the equivalent limit pressure $\boldsymbol{p^*_{le}}$ for the pressuremeter method, or the equivalent penetostatic resistance $\boldsymbol{q_{ce}}$ for the penetrometric method, surrounding an equivalent pile of length $\boldsymbol{L_{ef}}$.

Remember that the compressive bearing capacity $\boldsymbol{R_c}$ of an isolated deep foundation must be determined from the following general expression:

$$R_c = R_p + R_s = A_p q_{pl} + P \int_0^L q_s(z) dz \qquad [2]$$

R_p value of the peak resistance of the deep foundation;

R_s value of the axial friction resistance of the deep foundation;

A_p surface of the base of the deep foundation;

P the perimeter of the pile shaft;

L: the length of the foundation in the ground;

q_{pl} the value of the limit pressure at the pile tip;

$q_s(z)$ the value of the unitary axial friction limit at dimension z.

The Eurocode 7 standard can be used to calculate peak ultimate tensile stresses q_{pl} and axial limit friction q_s using pressuremeter or penetrometer methods.

III - CALCULATION OF THE VERTICAL DISPLACEMENT OF A PILE USING THE T-Z, Q-Z CURVE METHOD OR LOAD TRANSFER THEORY

III.1 - Principle of transfer curves

The transfer curve method is used to calculate the vertical displacement of a pile subjected to axial loading. It is based on the

progressive mobilization of the axial friction on the pile shaft τ or the stress under the pile base q_p with the relative soil-pile displacement s (Figure 3.a) . These curves are also known as ***t-z*** curves. The construction of these ***t-z*** curves is based on data collected during in-situ instrumented pile loading tests, laboratory tests on pile models, or from in-situ tests such as penetrometric or pressuremeter tests. According to this method, the soil/deep foundation interaction can be likened to a series of non-linear springs behaving independently of each other. The first ***t-z*** curves were developed by Coyle and Reese in 1966. A typical ***t-z*** curve is shown in Figure 2.

Noting ***P*** as the perimeter of the pile shaft, the equilibrium of a portion of pile (Figure 3.b) of infinitesimal dimension ***dz*** gives us the equation:

$$-\frac{N(z+dz)-N(z)}{dz} - P.\tau(s) = 0 \quad [3]$$

$$-\frac{dN(z)}{dz} - P.\tau(s) = 0 \quad [4]$$

For a pile element of length ***dz,*** Young's modulus E_P undergoing compressive stress $N(z)$the variation in length corresponding to the settlement undergone ds is given by:

$$ds = \Delta(dz) = -\frac{N(z)}{E_P A_P} dz \quad [5]$$

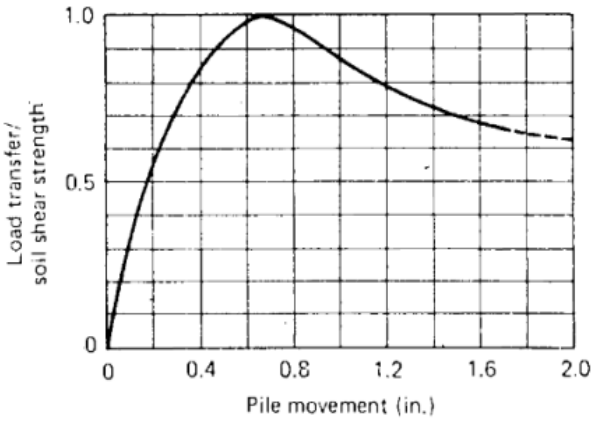

Figure 2. - Example of an axial friction mobilization curve (Coyle and Reese, 1966)

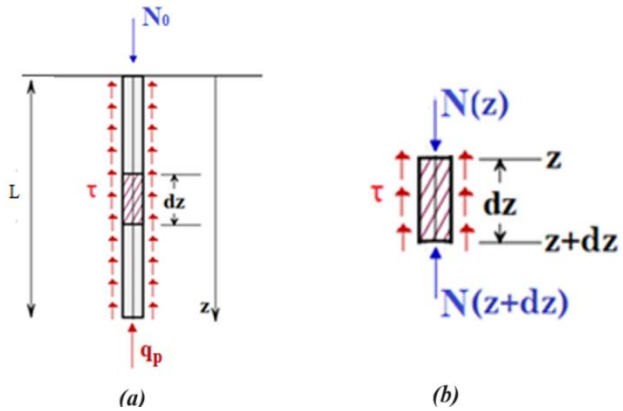

Figure 3 - (a) Pile under axial loading N_0 - (b) Pile section under normal stress N

We can thus write:

$$N(z) = -E_P A_P \frac{ds}{dz}. \quad [6]$$

By replacing the expression of $N(z)$ from equation (***6)*** into equation (***4)***, we obtain the differential equation for the equilibrium of a beam in compression. The transfer curve method is based on solving this equation:

$$E_P A_P \frac{d^2 s}{dz^2} - P.\tau(s) = 0 \quad [7]$$

For a pile with a circular cross-section of diameter ***D***, the equation becomes :

$$E_P A_P \frac{d^2 s}{dz^2} - \pi D\tau(s) = 0 \quad [8]$$

III.2 - Charge transfer parameters R_0 and B_0

The bearing capacity of a pile subjected to a vertical load results from the sum of the peak

resistance q_p and the lateral friction at the soil/pile interface. For low settlements, peak pressure and shear stress are defined by two parameters, R_0 and B_0 , which are used in load transfer theory to assess pile settlements. It is assumed that the stress mobilized at the soil/pile interface at a given depth is proportional to the settlement at that same depth:

$$\tau(z) = B_0(z)s(z) \quad [9]$$

$$q_p = R_0 \frac{s(L)}{D} \quad [10]$$

R_0 is the peak deformation parameter, representing the initial slope of the q_p curve as a function of $s(L)/D$ (Figure 4). This parameter can also be given directly in relation to $s(L)$ by setting the parameter $k_q = R_0/D$.

B_0also noted $k_\tau$is the mobilization parameter for lateral friction, and therefore represents the initial slope of the lateral friction curve as a function of settlement (Figure 5).

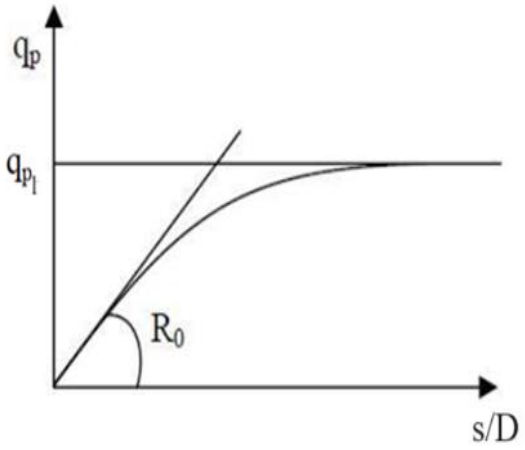

Figure 4. - Representation of the) q_p - s(L)/D curve (Bouafia, 2018

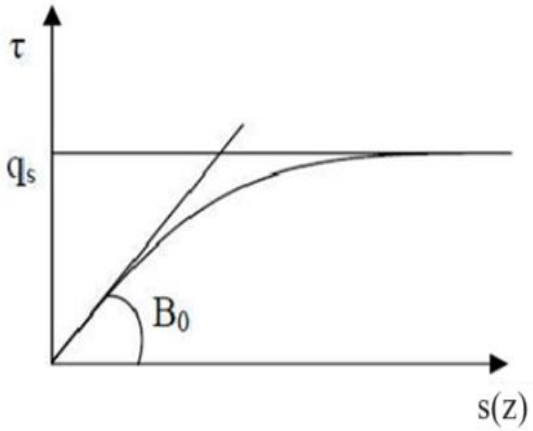

Figure 5. - Curve representation τ - s(z) (Bouafia, 2018)

In the case of a multi-layer soil or an inhomogeneous single-layer soil, where the profile $B_0(z)$ is arbitrary, the soil is broken down into a set of sufficiently thin slices such that it can be assumed that $B_0(z)$ is practically constant in a given segment of the pile, and ***equation 3*** can be integrated either by the finite-difference method, or by finding the analytical solution of this equation and imposing continuity at the interfaces of the slices. The latter procedure has been the basis of several computer programs such as PIVER and SETPIL (Bouafia, 2018).

IV. - ANALYTICAL CALCULATION OF SETTLEMENT, NORMAL FORCE AND DEFORMATION

IV.1. - Linear model by Verbrugge (1981)

For the Verbrugge model, the curves for axial friction mobilization τ***(s)*** and peak loading q_p ***(s_p)*** are linear. It is based on the results of penetrometric tests (Figure 6). The stiffness of the soil-pile interface is a function of the Young's modulus of the soil ***E*** and is calculated from the penetrometric peak resistance, the pile diameter D and the nature of the soil and pile type.

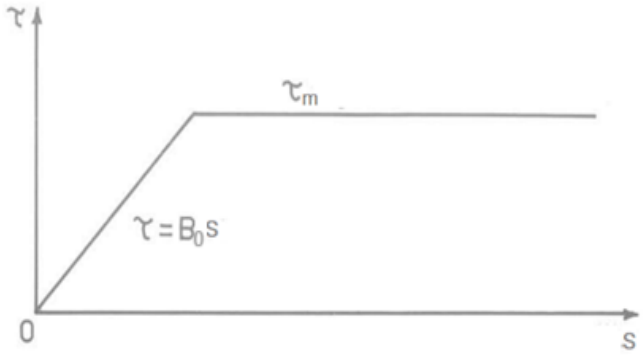

Figure 6. - Lateral friction mobilization law (Verbrugge, 1981)

The modulus of elasticity of the soil is given by the following relationship (*Verbrugge, 1981*):

$E(MPa) = 3{,}6 + 2{,}2q_c$ [11]

With q_c is the penetrometer tip resistance, in MPa.

The charge transfer parameter R_0 :

$R_0 = 3{,}125E$ [12]

Pile tip settlement:

$s_p = 0{,}32q_pD/E$ [13]

Axial friction law in the elastic domain

$\tau = B_0 s < \tau_m$ [14]

With :

$B_0 = 0{,}22\ E/D$ [15]

Verbrugge's law of friction in plastics $\tau = \tau_m$ [16]

IV.1.1. - Solving the pile equilibrium equation

The τ-s function is linearized as $\tau = A_0 + B_0 s$. Subsequently, a differential equation with constant coefficients is obtained whose analytical solution is given, depending on the value reached, by τ :

For $\tau = B_0 s < \tau_m$ the differential equation ***(8)*** becomes:

$E_P A_P \frac{d^2 s}{dz^2} - \pi D\tau = 0$ [17]

$E_P A_P \frac{d^2 s}{dz^2} - \pi D B_0 s = 0$ [18]

$\Rightarrow \frac{d^2 s}{dz^2} - \frac{\pi D B_0}{E_P A_P} s = 0$ [19]

Posing

$\boldsymbol{\mu^2 = \frac{\pi D B_0}{E_P A_P}}$ [20]

For a circular pile, we can write:

$\mu^2 = \frac{4B_0}{E_P D}$ [21]

$\Rightarrow \frac{d^2 s}{dz^2} - \mu^2 s = 0$ [22]

The equation can be written as $s'' - \mu^2 s = 0$. The general solution to this type of equation is:

$s(z) = a.\cosh(\mu z) + b.\sinh(\mu z)$ [23]

For $\tau_z = \tau_m$ the differential equation ***(8)*** becomes:

$E_P A_P \frac{d^2 s}{dz^2} - \pi D\tau_z = 0$ [24]

$E_P A_P \frac{d^2 s}{dz^2} - \pi D\tau_m = 0$ [25]

$\Rightarrow \frac{d^2 s}{dz^2} = \frac{\pi D\tau_m}{E_P A_P}$ [26]

By double integrating this equation, we find the analytical solution:

$\frac{d^2 s}{dz^2} = a + \frac{\pi D\tau_m}{E_P A_P} z$ [27]

$s = az + b + \frac{\pi D\tau_m}{E_P A_P} \frac{z^2}{2}$ [28]

$\boldsymbol{s(z) = az + b + \frac{\pi D\tau_m}{E_P A_P} \frac{z^2}{2}}$ [29]

IV.1.2. - Determination of constants a and b

The integration constants are determined by the boundary conditions or the conditions at the interface of the layers (continuity of the normal force N_z and s_z). Let's consider a free pile of length L at the head subjected to a normal force N_0 for a settlement at the head s_0 and at the tip s_p .

For: $s(z) < \frac{\tau_m}{B_0}$ et $\tau_z < \tau_m$

Stake head : $z = 0$

$s(0) = s_0 = a\cosh(0) + b\sinh(0)$. We obtain

$\boldsymbol{s_0 = a}$ [30]

From equation (5), we can therefore say :

$\frac{ds(z)}{dz} = a\mu\sinh(\mu z) + b\mu\cosh(\mu z) = -\frac{N(z)}{E_P A_P}$ [31]

Assuming $N_0$the value of the axial force at the head of the pile (z = 0), we obtain :

$-a\mu\sinh(0) + b\mu\cosh(0) = -\frac{N(0)}{E_P A_P}$ [32]

and we draw $\boldsymbol{b} = -\frac{\boldsymbol{N_0}}{\boldsymbol{\mu E_P A_P}}$ [33]

The compaction expression gives :

$s(z) = \cosh(\mu z)\boldsymbol{s_0} - \frac{\sinh(\mu z)}{\mu E_P A_P}\boldsymbol{N_0}$. [34]

From this, we can deduce the evolution of the **axial** force $N(z)$ with equation (6) and also define the expression for relative axial deformation given by :

$\varepsilon(z) = \frac{N(z)}{E_P A_P} = -\frac{ds(z)}{dz}$. [35]

This gives us the following system:

$$\begin{cases} \boldsymbol{s(z) = \cosh(\mu z) s_0 - \frac{\sinh(\mu z)}{\mu E_P A_P} N_0} \\ \boldsymbol{N(z) = -E_P A_P \mu \sinh(\mu z)\, s_0 + \cosh(\mu z)\, N_0} \\ \boldsymbol{\varepsilon(z) = -\sinh(\mu z)\, s_0 + \frac{\cosh(\mu z)}{E_P A_P} N_0} \end{cases} \quad \textbf{[36]}$$

Pile point: $z = L$

From equation (5) and (10), we can write :

$\frac{ds(z=L)}{dz} = -\frac{N(z=L)}{E_P A_P} = -\frac{q_p}{E_P} = -\frac{R_0 s(z=L)}{E_P D}$ [37]

$\frac{ds(L)}{dz} = -\frac{R_0}{E_P D} s(L)$ [38]

$\Rightarrow \mu \sinh(\mu L)\, s_0 - \frac{\cosh(\mu L)}{E_P A_P} N_0 = -\frac{R_0}{E_P D}\left(\cosh(\mu L) s_0 - \frac{\sinh(\mu L)}{\mu E_P A_P} N_0\right)$ [39]

Dividing both members by $\cosh(\mu L)$ gives :

$\mu \tanh(\mu L)\, s_0 - \frac{N_0}{E_P A_P} = -\frac{R_0}{E_P D}\left(s_0 - \frac{\tanh(\mu L)}{\mu E_P A_P} N_0\right)$ [40]

$s_0\left[\mu \tanh(\mu L) + \frac{R_0}{E_P D}\right] = \frac{N_0}{E_P A_P} + \frac{R_0 N_0}{E_P D}\frac{\tanh(\mu L)}{\mu E_P A_P}$ [41]

By multiplying both members by $E_P D$ and posing $A_P = \frac{\pi D^2}{4}$

$s_0[R_0 + \mu E_P D \tanh(\mu L)] = \frac{4N_0}{\pi D} + \frac{4N_0}{\pi D}\frac{R_0 \tanh(\mu L)}{\mu E_P D}$ [42]

This resolution allows us to write the settlement at the head of the pile s_0 as a function of the axial force applied at the head N_0. We derive the settlement at the head of the pile for settlements $s(z) < \frac{\tau_m}{B_0}$:

$$\boldsymbol{s_0 = \frac{4N_0}{\pi D}\frac{1+\frac{R_0 \tanh(\mu L)}{\mu D E_P}}{R_0 + \mu D E_P \tanh(\mu L)}} \quad \textbf{[43]}$$

For $s(z) \geq \frac{\tau_m}{B_0}$ et $\tau = \tau_m$equation (29) gives

$s(z) = az + b + \frac{\pi D \tau_m}{E_P A_P}\frac{z^2}{2}$

Stakehead: $z = 0$

$s(0) = s_0 \Rightarrow \boldsymbol{b = s_0}$ [44]

From equation (5), we derive :

$\frac{ds(z)}{dz} = a + \frac{\pi D \tau_m}{E_P A_P} z = -\frac{N(z)}{E_P A_P}$ [45]

For $z = 0$, $a = -\frac{N(0)}{E_P A_P} \Rightarrow \boldsymbol{a = -\frac{N_0}{E_P A_P}}$ **[46]**

Therefore, the expression for settlement

$s(z) = \boldsymbol{s_0} - \frac{z}{E_P A_P}\boldsymbol{N_0} - \frac{\pi D \tau_m}{E_P A_P}\frac{z^2}{2}$ [47]

The expressions for $N(z)$ and $\varepsilon(z)$ from equations (6) and (35):

$$\begin{cases} \boldsymbol{s(z) = s_0 - \frac{z}{E_P A_P} N_0 + \frac{\pi D \tau_m}{E_P A_P}\frac{z^2}{2}} \\ \boldsymbol{N(z) = N_0 - \pi D \tau_m z} \\ \boldsymbol{\varepsilon(z) = \frac{N_0}{E_P A_P} - \frac{\pi D \tau_m}{E_P A_P} z} \end{cases} \quad [48]$$

Pile point: $z = L$

From equation (38), we can write:

$\Rightarrow -\frac{N_0}{E_P A_P} + \frac{\pi D \tau_m}{E_P A_P} L = -\frac{R_0}{E_P D}\left(s_0 - \frac{N_0 L}{E_P A_P} + \frac{\pi D \tau_m}{E_P A_P}\frac{L^2}{2}\right)$ [49]

This gives the expression for head settlement s_0 for settlement values $s(z) \geq \frac{\tau_m}{B_0}$

$$\boldsymbol{s_0 = \frac{N_0 L}{E_P A_P} + \frac{4N_0}{\pi D R_0} - 4\tau_m L\left[\frac{L}{2E_P D} + \frac{1}{R_0}\right]} \quad \textbf{[50]}$$

IV.2 - Frank and Zhao (1982) trilinear model

Frank and Zhao's (1982) model for axial friction mobilization $\boldsymbol{\tau(s_z)}$ and peak loading $\boldsymbol{q_p}$ $\boldsymbol{(s_p}$) is trilinear and is based on pressuremeter results (Figure 7). The stiffness of the soil-pile interface is a function of the soil pressure modulus E_M, the pile diameter D and the nature of the soil (fine or granular soils). By comparison with Verbrugge's linear model, Frank and Zhao add an intermediate domain of behavior that can be considered as the elastoplastic domain. The initial slopes k_τ and k_q are given respectively for fine (clays and silts) and granular soils by the relationships:

For fine soil:

$k_\tau = 2E_M/D$; $k_q = 11E_M/D$ [51]

For granular soil

$k_\tau = 0{,}8E_M/D$; $k_q = 4{,}8E_M/D$ [52]

Where:

E_M Pressuremeter modulus at the depth in question;

D: Pile diameter.

Since this study concerns clay soils, we will focus on the values of k_τ and k_q for fine soils.

Frank and Zhao (1982) give the mobilization laws for friction τ *as a* function of vertical displacement *s* of the pile in each section and the modeling law for peak force q_p as a function of vertical displacement s_p.

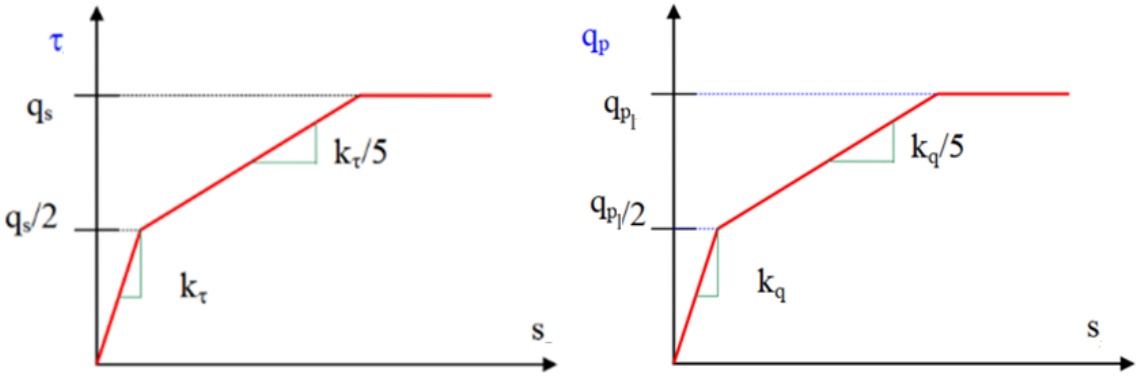

Figure 7. - Mobilization law for lateral friction and unit peak force (Frank and Zhao 1982)

According to Frank and Zhao, each curve is made up of *three segments:*

The first has a constant slope (k_τ or k_q) until 50% of the limit value (q_p (s_p) or $\tau(s)$) is mobilized.

$$\textit{Stage 1:}\begin{cases}\tau_1 = \frac{q_s}{2} \text{ et } s_1 = \frac{q_s/2}{k_\tau} \\ q_{p_1} = \frac{q_{pl}}{2} \text{ et } s_{p_1} = \frac{q_{pl}/2}{k_q}\end{cases} \quad [53]$$

The second segment has a constant slope up to the limit value and is equal to 1/5 of that of the first segment (k_τ/5 or k_q/5)

$$\textit{Stage 2:}\begin{cases}\tau_2 = q_s \text{ et } s_2 = \frac{q_s/2}{k_\tau} + \frac{q_s/2}{\frac{k_\tau}{5}} \\ q_{p_2} = q_{pl} \text{ et } s_{p_2} = \frac{q_{pl}/2}{k_p} + \frac{q_{pl}/2}{\frac{k_p}{5}}\end{cases} \quad [54]$$

The third segment corresponds to the complete mobilization of axial friction or peak resistance.

The function $\tau(s)$ is linearized as $\tau = A_0 + B_0 s$. Based on the *trilinear* mobilization law for axial friction, we can find the values of A_0 and B_0 (Table 3) for each phase. These values are a function of the mechanical characteristics of the soil layers. The expression for unit friction τ can be deduced for fine soils (Table 3).

IV.2.1. - Resolution of the pile equilibrium equation using the Frank and Zhao trilinear model

The τ-s function is linearized as $\tau = A_0 + B_0 s$. Thus a differential equation with constant coefficients is obtained whose analytical solution is given according to the values of A_0 et B_0 (Table 1).

Table 1. - Expression of mobilized lateral friction τ for each bearing

Expressions of τ (fine soils : $k_\tau = 2E_M/D$)		
Bearing N°1	**Level N°2**	**Horizontal bearing**
$\text{Si } 0 \le s \le \frac{q_s}{2k_\tau}$ $\Leftrightarrow \text{Si } 0 \le s \le \frac{q_s D}{4E_M}$	$\text{Si } \frac{q_s}{2k_\tau} \le s \le \frac{3q_s}{k_\tau}$ $\Leftrightarrow \text{Si } \frac{q_s D}{4E_M} \le s \le \frac{3q_s D}{2E_M}$	$\text{Si } s \ge \frac{3q_s}{k_\tau}$ $\Leftrightarrow \text{Si } s \ge \frac{3q_s D}{2E_M}$
$A_0 = 0$ et $B_0 \neq 0$	$A_0 \neq 0$ et $B_0 \neq 0$	$A_0 \neq 0$ et $B_0 = 0$

$\tau = B_0 s = k_\tau s$	$\tau = A_0 + B_0 s = \frac{2q_s}{5} + \frac{k_\tau}{5} s$	$\tau = A_0 = q_s$
$A_0 = 0$ et $B_0 = k_\tau$	$A_0 = \frac{2q_s}{5}$ et $B_0 = \frac{k_\tau}{5}$	$A_0 = q_s$ et $B_0 = 0$
$\Longrightarrow A_0 = 0$ et $B_0 = 2E_M/D$	$A_0 = \frac{2q_s}{5}$ et $B_0 = \frac{2E_M}{5D}$	$A_0 = q_s$ et $B_0 = 0$
$\tau = \frac{2E_M}{D} s$	$\tau = \frac{2q_s}{5} + \frac{2E_M}{5D} s$	$\tau = q_s$

For $A_0 = 0$ et $B_0 = 2E_M/D$:

$0 \le s(z) \le \frac{q_s D}{4E_M}$ et $\tau \le \frac{q_s}{2}$

The differential equation ***(8)*** becomes :

$$\frac{d^2 s}{dz^2} - \frac{\pi D B_0}{E_P A_P} s = 0 \quad [55]$$

With $\boldsymbol{\mu^2 = \frac{\pi D B_0}{E_P A_P}}$ $\Rightarrow \frac{d^2 s}{dz^2} - \mu^2 s = 0$ [56]

The general solution of this equation is :

$$s(z) = a.\cosh(\mu z) + b.\sinh(\mu z) \quad \textbf{[57]}$$

For $A_0 = \frac{2q_s}{5}$ et $B_0 = \frac{2E_M}{5D}$:

$\frac{q_s D}{4E_M} \le s(z) \le \frac{3q_s D}{2E_M}$ et $\frac{q_s}{2} \le \tau \le q_s$

The differential equation ***(8)*** becomes :

$$E_P A_P \frac{d^2 s}{dz^2} - \pi D(A_0 + B_0 s) = 0 \quad [58]$$

$$\frac{d^2 s}{dz^2} - \frac{\pi D B_0}{E_P A_P} s = \frac{\pi D A_0}{E_P A_P} \quad [59]$$

The equation can be written as :

$$s'' - \mu^2 s = \mu^2 \frac{A_0}{B_0} \quad [60]$$

The general solution of this type of equation is the sum of the solution without a second member and the so-called particular solution. The general solution without second member of this equation is :

$$s_g = a.\cosh(\mu z) + b.\sinh(\mu z) \quad [61]$$

Since the second member of this equation is a constant, the particular solution is a constant which we will note s_{pa} and is obtained by solving the equation $s_{pa}'' - \mu^2 s_{pa} = \mu^2 \frac{A_0}{B_0}$.

s_{pa} = constante $\Rightarrow s_{pa}'' = 0$, we obtain :

$$-\mu^2 s_{pa} = \mu^2 \frac{A_0}{B_0} \Rightarrow s_{pa} = -\frac{A_0}{B_0} \quad [62]$$

The general solution of the differential equation $s = s_g + s_{pa}$. We therefore obtain :

$$\boldsymbol{s(z) = a.\cosh(\mu z) + b.\sinh(\mu z) - \frac{A_0}{B_0}} \quad \textbf{[63]}$$

For $A_0 = q_s$ et $B_0 = 0$, $\tau = A_0$:

$s(z) \ge \frac{3q_s D}{2E_M}$ et $\tau = q_s$

The differential equation (***8***) becomes:

$$E_P A_P \frac{d^2 s}{dz^2} - \pi D A_0 = 0 \quad [64]$$

$$\Rightarrow \frac{d^2 s}{dz^2} = \frac{\pi D A_0}{E_P A_P} \quad [65]$$

By double integrating this equation, we find the analytical solution:

$$\frac{d^2 s}{dz^2} = a + \frac{\pi D A_0}{E_P A_P} z \quad [66]$$

$$s = az + b + \frac{\pi D A_0}{E_P A_P} \frac{z^2}{2} \quad [67]$$

$\boldsymbol{\tau}$ is equal to the value of the limiting unit axial friction q_s ($\tau = A_0 = q_s$);

$$\boldsymbol{s(z) = az + b + \frac{\pi D q_s}{E_P A_P} \frac{z^2}{2}} \quad \textbf{[68]}$$

IV.2.2. - Determination of constants a and b

The integration constants are determined from the boundary conditions. Let's consider a free pile of length *L* subjected at the head to a normal force $\boldsymbol{N_0}$ for a settlement of $\boldsymbol{s_0}$ at the head and $\boldsymbol{s_p}$ at the tip.

For $0 \le s(z) \le \frac{q_s D}{4E_M}$ et $\tau \le \frac{q_s}{2}$,

$s(z) = a\cosh(\mu z) + b\sinh(\mu z)$

Stakehead : $z = 0$ *and* $s(z = 0) = s_0$

Using equations (6) and (35), we can demonstrate and write the following system:

$$\begin{cases} \boldsymbol{s(z) = \cosh(\mu z) s_0 - \frac{\sinh(\mu z)}{\mu E_P A_P} N_0} \\ \boldsymbol{N(z) = -E_P A_P \mu \sinh(\mu z)\, s_0 + \cosh(\mu z)\, N_0} \\ \boldsymbol{\varepsilon(z) = -\mu \sinh(\mu z)\, s_0 + \frac{\cosh(\mu z)}{E_P A_P} N_0} \end{cases} \quad \textbf{[69]}$$

Pile point: $z = L$

From the relationship $q_p = R_0 s(L)/D$ and equation (5), we can write pile-head settlement s_0 as a function of the axial force applied at the head N_0 given by :

$$\boldsymbol{s_0 = \frac{4N_0}{\pi D} \frac{1 + \frac{R_0 \tanh(\mu L)}{\mu D E_P}}{R_0 + \mu D E_P \tanh(\mu L)}} \quad \textbf{[70]}$$

For $\frac{q_s D}{4E_M} \le s(z) \le \frac{3q_s D}{2E_M}$ et $\frac{q_s}{2} \le \tau \le q_s$,

$$s(z) = a.\cosh(\mu z) + b.\sinh(\mu z) - \frac{A_0}{B_0}$$

Stakehead : $z = 0$

$\Rightarrow s(0) = a.\cosh(0) + b.\sinh(0) - \frac{A_0}{B_0}$

$\Rightarrow s_0 = a - \frac{A_0}{B_0} \Rightarrow \boldsymbol{a = s_0 + \frac{A_0}{B_0}}$ [71]

From equation (5), we derive :

$\frac{ds(z)}{dz} = a\mu\sinh(\mu z) + b\mu\cosh(\mu z) = -\frac{N(z)}{E_P A_P}$ [72]

For $z = 0$, $a\mu\sinh(0) + b\mu\cosh(0) = -\frac{N(0)}{E_P A_P}$.

We draw $\boldsymbol{b = -\frac{N_0}{\mu E_P A_P}}$ [73]

Therefore, the expression for settlement $s(z) = \cosh(\mu z)\left(s_0 + \frac{A_0}{B_0}\right) - \frac{\sinh(\mu z)}{\mu E_P A_P} N_0 - \frac{A_0}{B_0}$. [74]

The expression for $\boldsymbol{N(z)}$ and also $\boldsymbol{\varepsilon(z)}$ with equation (35). The following system is obtained:

$$\begin{cases} \boldsymbol{s(z) = \cosh(\mu z)\, s_0 - \frac{\sinh(\mu z)}{\mu E_P A_P} N_0 + \frac{A_0}{B_0}(\cosh(\mu z) - 1)} \\ \boldsymbol{N(z) = -E_P A_P \mu \sinh(\mu z)\, s_0 + \cosh(\mu z)\, N_0 - \frac{E_P A_P A_0 \mu}{B_0}\sinh(\mu z)} \\ \boldsymbol{\varepsilon(z) = -\mu \sinh(\mu z)\, s_0 + \frac{\cosh(\mu z)}{E_P A_P} N_0 - \frac{A_0 \mu}{B_0}\sinh(\mu z)} \end{cases} \quad \textbf{[75]}$$

In pile point: $z = L$ with equations (5) and (10),

We can write $\frac{ds(L)}{dz} = -\frac{R_0}{E_P D} s(L)$ [76]

It is easy to see that the settlement at the head of the pile is given by:

$\boldsymbol{s_0 = \frac{4N_0}{\pi D}\frac{1+\frac{R_0\tanh(\mu L)}{\mu D E_P}}{R_0 + \mu D E_P \tanh(\mu L)} + \frac{A_0}{B_0}\left(\frac{R_0}{R_0\cosh(\mu z) - \mu D E_P \sinh(\mu z)} - 1\right)}$ **[77]**

For $s(z) \geq \frac{3q_s D}{2E_M}$ *et* $\tau = q_s$,

$s(z) = az + b + \frac{\pi D q_s}{E_P A_P}\frac{z^2}{2}$

Stakehead: $z = 0 \Rightarrow s(0) = \boldsymbol{b = s_0}$

From equation (***5***), we derive $\boldsymbol{a = -\frac{N_0}{E_P A_P}}$

The expressions for $N(z)$ and $\varepsilon(z)$ with equations (***5***) and (***35***), giving the following system:

$$\begin{cases} \boldsymbol{s(z) = s_0 - \frac{z}{E_P A_P} N_0 + \frac{\pi D q_s}{E_P A_P}\frac{z^2}{2}} \\ \boldsymbol{N(z) = N_0 - \pi D q_s z} \\ \boldsymbol{\varepsilon(z) = \frac{N_0}{E_P A_P} - \frac{\pi D q_s}{E_P A_P} z} \end{cases} \quad \textbf{[78]}$$

Pile point: $z = L$

From equation (**76**), we can solve and write the expression for head settlement s_0 for settlement values $s(z) \geq \frac{3q_s D}{2E_M}$

$\boldsymbol{s_0 = \frac{N_0 L}{E_P A_P} + \frac{4N_0}{\pi D R_0} - 4q_s L\left[\frac{L}{2E_P D} + \frac{1}{R_0}\right]}$ **[79]**

IV.3. - Hyperbolic model by Hirayama (1990)

Hirayama (1990) assumes that the mobilization laws for lateral friction τ and peak force q_p as a function of displacement s are hyperbolic laws of the Kondner type (Figure 8).

$\tau = \frac{s}{a_f + b_f s}$ [80]

$q_p = \frac{s_p}{a_e + b_e s_p}$ [81]

Where a_f, b_f, a_e and b_e are constants.

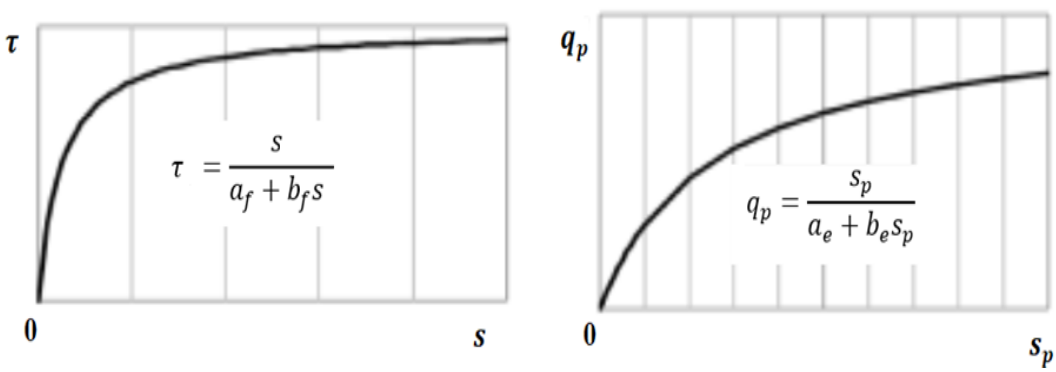

Figure 8. - Mobilization law for lateral friction and unit peak force Hirayama (1990)

The principle of Hirayama's method is to determine these 4 constants, on the one hand, using the limiting forces q_s and q_{p_l} on the pile, and secondly, by knowing typical displacement values at 50% of the mobilization of these limit forces.

IV.3.1. - Determination of a_f, b_f, a_e and b_e

The constants b_f and b_e are determined by :

$$b_f = 1/q_s \quad [82]$$

$$b_e = 1/q_{p_l} \quad [83]$$

The usual methods for estimating q_s and q_{p_l} can be used.

The constant a_f is the slope of the initial tangent of the curve τ-s. This tangent is not easy to determine, as it is very sensitive to soil reworking. Hirayama suggests determining it from q_s and the displacement $s_{ref,f}$ for which half of q_s is mobilized. Reese (1978) estimates that, for both clays and sands, the limiting lateral friction q_s is mobilized when s is between 0.5% and 2% of the pile shaft diameter D. On this basis, and on the basis of data from other authors, Hirayama retains :

$s_{ref,f} \approx 0{,}0025\text{D}$; a_f is then given by: $a_f = 0{,}0025\, D/q_s$ [84]

$\boldsymbol{a_e}$ is determined by the displacement $s_{ref,e}$ equivalent to the mobilization of half of q_{p_l}. Taking into account the work of Meyerhof (1956) and Reese (1978), Hirayama uses $s_{ref,e} \approx 0{,}25\text{D}$ to give $a_e = 0{,}25\, D/q_{p_l}$. [85]

The author also notes that the values of $s_{ref,f}$ (for lateral friction) are smaller than those of $s_{ref,e}$ (for peak force), which seems normal.

IV.3.2. - Solving the pile equilibrium equation using Hirayama's hyperbolic model

The function τ is hyperbolic. By replacing it in equation (8), we can develop the following differential equation:

$$\frac{d^2s}{dz^2} - \frac{\pi D}{E_P A_P}\left(\frac{s}{a_f + b_f s}\right) = 0 \quad [86]$$

This differential equation is nonlinear of the second order. To solve this equation, we can use the order reduction method by positing a function

$$x(z) = \frac{d^2s}{dz^2}. \quad [87]$$

The equation thus becomes a system of two first-order differential equations.

The result is $\frac{dx}{dz} = \frac{d^2s}{dz^2}$. The system of equations becomes :

$$\begin{cases} x(z) = \frac{d^2s}{dz^2} \\ \frac{dx}{dz} = \frac{\pi D}{E_P A_P}\left(\frac{s}{a_f + b_f s}\right) \end{cases} \quad [88]$$

This system of equations can be solved for $s(z)$ and $x(z)$. However, the explicit solution may be complex depending on the specific values of D, E_P, A_P, a_f and b_f. To obtain a more precise solution, it will be necessary to specify the values of these parameters.

IV.4. - Exponential model of Abchir and Burlon (AB1, 2016)

IV.4.1. - Principle of the exponential law AB1

Abchir and Burlon proposed a hyperbolic curve for the ***t-z*** curves, to suppress discontinuous variations in the shear stress mobilization slope. They considered that soil stiffness at the soil-pile interface is proportional to the difference between the limiting axial friction q_s and the mobilized axial friction τ (***q_s - τ***).

$$\frac{d\tau}{ds} = \frac{q_s - \tau}{\lambda_s} \quad [89]$$

Withτ the mobilized axial friction, q_s the limiting axial friction, s the pile settlement at depth z :

$$\tau(s) = q_s(1 - e^{-\frac{s}{\lambda_s}}). \quad [90]$$

The evolution of peak resistance is expressed by: $q_p(s_p) = q_{p_l}(1 - e^{-\frac{s_p}{\lambda_p}})$. [91]

With:

$$\lambda_s = q_s/k_s \quad [92]$$

$$\lambda_p = q_{p_l}/k_p \quad [93]$$

Where k_s is the initial stiffness of the ***t-z*** curve and is equal to k_τ from the ***Frank and Zhao*** model ; $k_p$is the initial stiffness of the ***q*** curve***p*** - ***s*****p** and is equal **to** k_q of the ***Frank and Zhao*** model.

Figure 9 shows the ***t-z*** curve and its rigidity according to model ***AB1***.

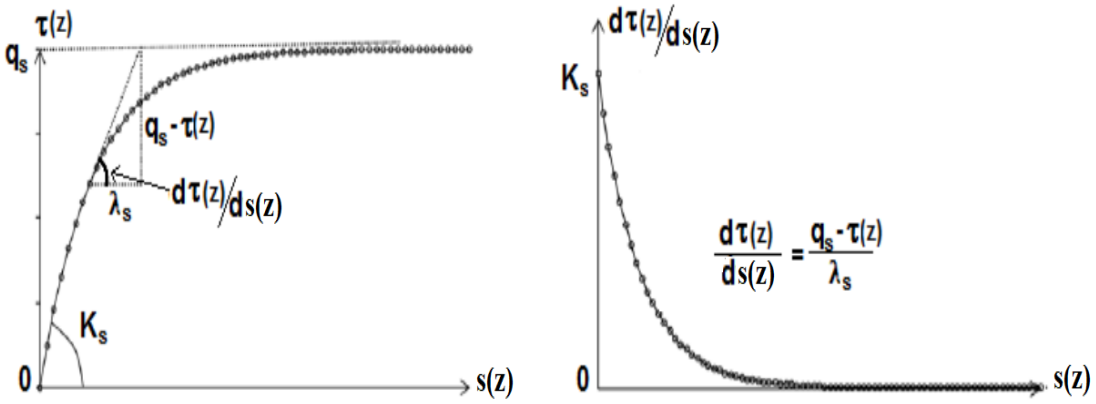

Figure 9. - t-z curve and stiffness of AB1 model (2016)

IV.4.2. - Solving the pile equilibrium equation using Abchir and Burlon's exponential model

The function τ is exponential. By replacing τ in equation (4.5), we can develop the following differential equation:

$$\frac{d^2s}{dz^2} - \frac{\pi D q_s}{E_P A_P}\left(1 - e^{-\frac{k_s}{q_s}s}\right) = 0 \qquad [94]$$

We find a second-order non-linear differential equation. The exact solution $s(z)$ depends on the specific values of the parameters E_P, A_P, q_s, D and k_s.

In the following, we will present a comparative study of these different laws on the behavior of the pile subjected to axial loading.

V. - COMPARATIVE STUDY OF DIFFERENT BEHAVIOR LAWS

V.1 - Comparison of t-z curves

Verbrugge's linear law is based on the results of the penetrometric test, in particular on the value of the cone's penetration resistance $\boldsymbol{q_c}$. Frank and Zhao's trilinear, Hirayama's hyperbolic and AB1's exponential laws are based on the results of the pressuremeter test, in particular on the value of the resistance limit lateral friction $\boldsymbol{q_s}$. The ***t-z*** curves defining the soil-pile interaction laws for a clay soil mass are constructed on the basis of the penetrometer-pressiometer correlations for clay soils by Cassan (1978):

$$E_M/q_c = 3{,}3 \qquad [95]$$

Let's consider a bored pile with diameter D = 0.8 m, length L = 20 m in clay with pressure modulus E_M = 5 MPa for a limit pressure *pl* = 0.42 MPa. The lateral friction limit obtained q_s= 0.038 MPa, cone penetration resistance q_c= 1.515 MPa. For this resistance value q_cVerbrugge's limiting lateral friction is given by the following formula:

$$\tau_m = 0{,}015 q_c \qquad [96]$$

Figure 10 illustrates the various characteristic ***t-z*** curves for a given clay soil and pile type. In general, in pressuremeter models, the shape of the curve describing the mobilization of axial friction directly takes into account the limiting value q_s ***Frank and Zhao***'s model generally mobilizes a higher level of axial friction than the ***AB1*** and ***Hirayama models*** for a given displacement.

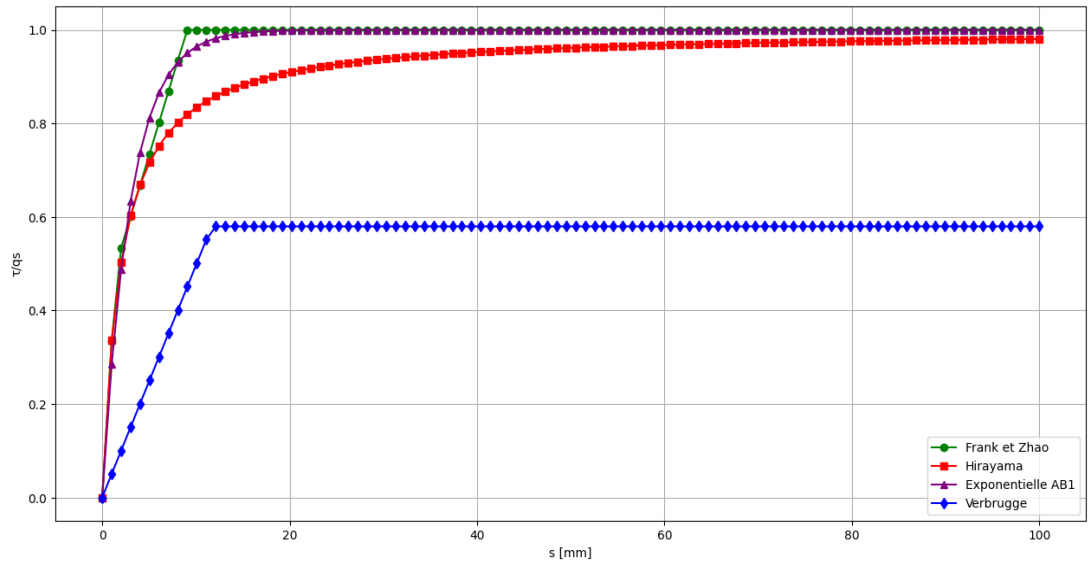

Figure 10. - Comparison of t-z curves for the four models

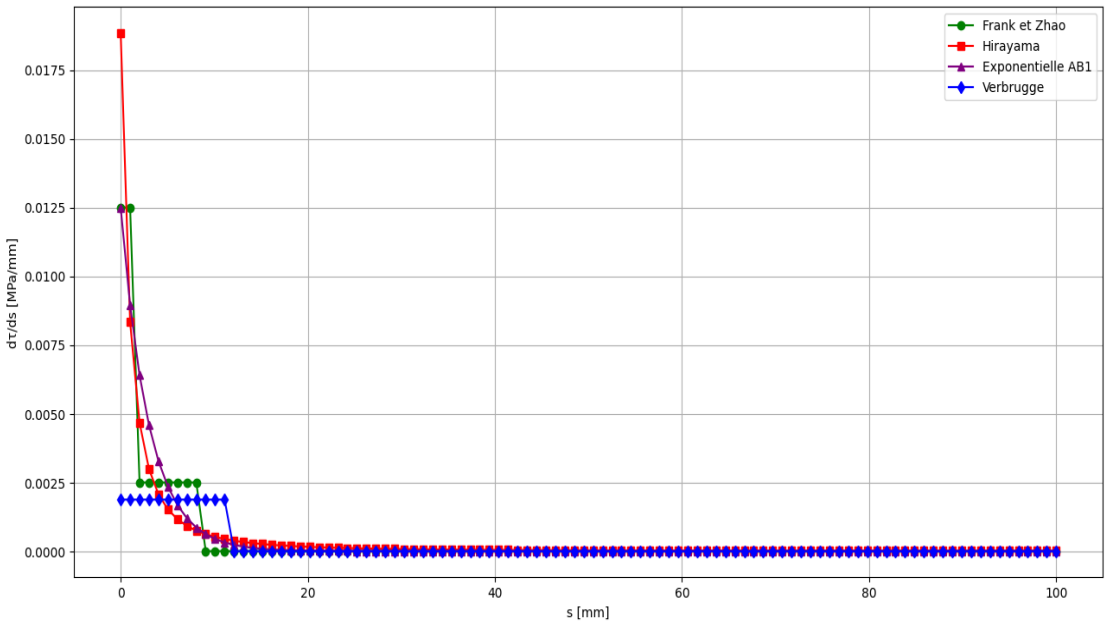

Figure 11. - Comparison of soil stiffness curves at the soil-pile interface according to the four previous models

In other words, the results show that the Frank and Zhao model is steeper than the other two. We also note that friction mobilization according to the Frank and Zhao and AB1 models can reach the limiting unit friction value q_s. This is not the case with Hirayama's model, where mobilized friction always remains strictly below q_s. A clear difference can be seen in the Verbrugge model, which has a lower mobilization of unit lateral friction. Moreover, the complete mobilization of lateral friction according to Verbrugge, corresponding here to friction in the plastic domain τ_m is lower than in the case of pressuremeter models when lateral friction reaches the limit value q_s. Depending on the parameter values used, and taking into account the Cassan correlation, we obtain $\tau_m = 0{,}58\ q_s$. This means that pressuremeter models offer a 40% gain in terms of lateral friction mobilization over the Verbrugge model.

Figure 11 shows the evolution of soil stiffness ***dτ/ds*** *as a* function of pile settlement according to several models. It is clear that, for the Verbrugge and Frank &

Zhao models, the evolution of stiffness at the soil-pile interface is discontinuous, whereas it remains continuous for the AB1 and Hirayama models. A distinct feature is observed in the Hirayama model, where the final soil stiffness does not tend towards zero. This is due to the fact that mobilized friction is always strictly below the limit value, and axial friction is not limited by a fixed value. q_s.

V.2. - Comparison of settlement, normal force and deformation curves

Consider a bored pile with diameter ***D*** equal to 0.8 m, length L = 20 m in clay with pressure modulus E_M equal to 5 MPa and limit pressure ***pl*** equal to 0.42 MPa. The lateral friction limit obtained q_s = 0.038 MPa, cone penetration resistance q_c derived from the Cassan correlation is equal to 1.515 MPa and we deduce the Verbrugge Young's modulus E (***Eq. 11***) and its plastic deformation law τ_m(***Eq. 96***). The pile is made of concrete with a characteristic strength f_{ck} equal to 25 MPa and Young's modulus E_p modulus of 10.49 MPa.

Once these input parameters have been set, the non-linear second-order differential equations of Verbrugge and Hirayama can be solved using the Python programming language, with its libraries for scientific computing (*Numpy*, *Scipy*, *Math*) and graphical visualization (*Matplotlib)*; this enables us to carry out a numerical resolution and plot the various curves for the evolution of settlement, normal stress and relative deformation according to the four models studied in this comparative behavior study.

In this comparative study, the pile is subjected to a load N_0 equal to 0.9 MN and pile head settlement s_0 equal to 3 mm. In order to make the results more applicable and accessible, the values are made dimensionless.

Relative settlement is represented as $(s(z)/s_0)$ relative normal stress $(N(z)/N_0)$ and relative deformation $\varepsilon(z)$ as a function of the ratio of pile depth to length (z/L).

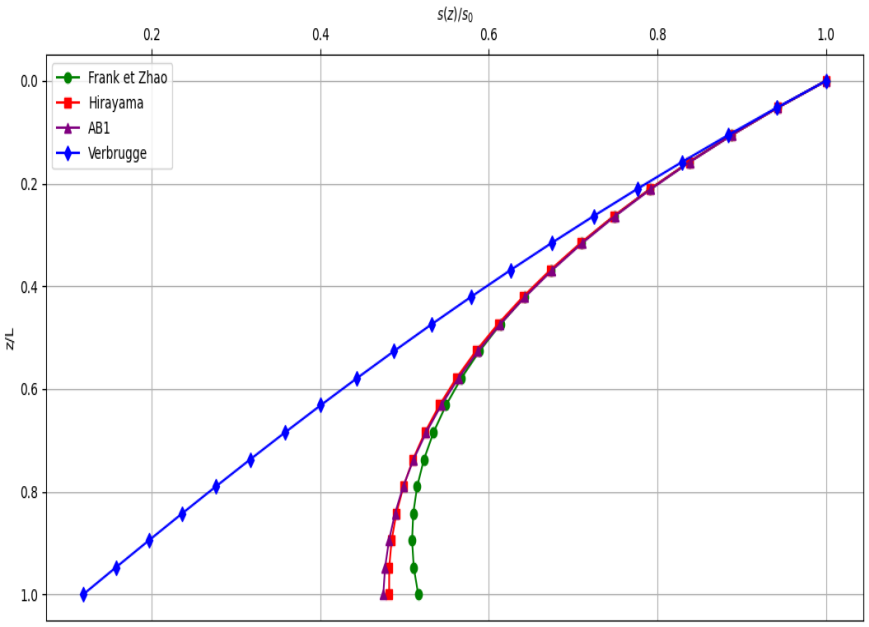

Figure 12. - Comparison of settlement trends for the four models

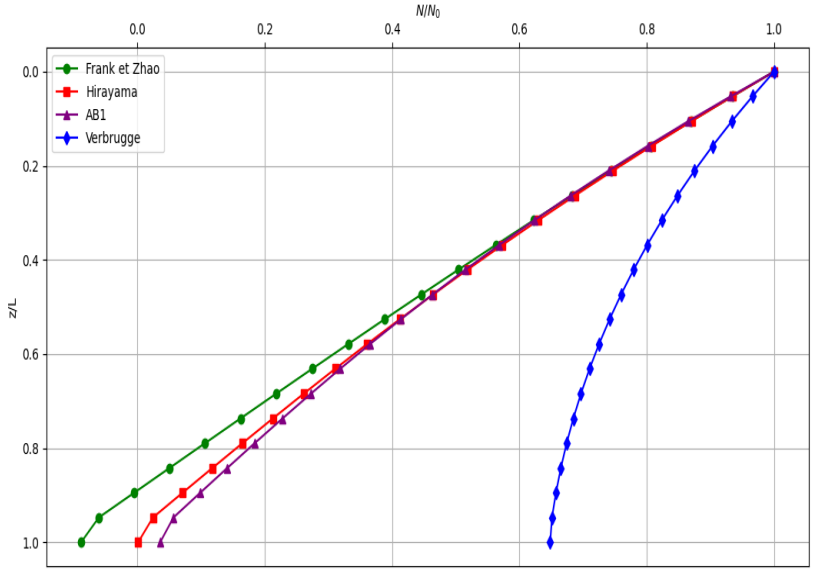

Figure 13. - Comparison of normal force evolution according to the four models

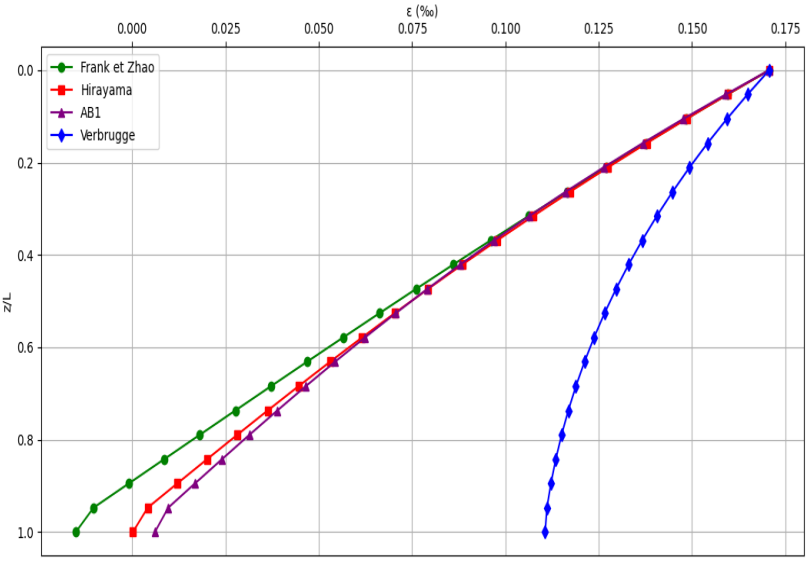

Figure 14. - Comparison of the evolution of relative strain according to the four models

These results, presented in figures 12, 13 and 14, confirm the remarks made in the comparative study of the four behavioral models concerning the mobilization of lateral friction around the pile. $\tau(s)$. The pressuremeter models mobilize more lateral friction for a given displacement, so we can understand a more obvious decrease in normal force at depth. The results show that the normal force following the Frank and Zhao model decreases faster. The same applies to relative deformation $\boldsymbol{\varepsilon}$ which, for constant longitudinal pile stiffness $(E_p A_p)$ the same hyperbolic shape as normal stress. With regard to settlement, the decrease in depth is very significant with the Verbrugge model. The evolution curves obtained with pressuremeter models, in particular that of Frank and Zhao, show a more acceptable evolution. This can be explained by the greater stiffness of these models and the greater mobilization of lateral friction around the pile.

VI. - CONCLUSION

This study explored in detail the behavior of a pile subjected to axial loading through the analysis of axial deformations, normal forces, and the complex interactions between the pile and the surrounding soil. Using the load transfer curve method, several behavior models were examined, each based on linear

trilinear, root function, hyperbolic or exponential laws.

The results of this study show that behavior models vary in their ability to predict settlement and axial stress, depending on the specific characteristics of the soil and the pile. Among the ***t-z*** and ***q-z*** models examined, pressuremeter models, such as those developed by Frank and Zhao, proved particularly effective in predicting pile behavior in clay soils, offering a better match with experimental results.

This work highlights the importance of choosing a behavioral model adapted to the specific geotechnical context, in order to guarantee accurate predictions and optimize foundation design. In addition, the integration of numerical simulations is also a promising approach to improving the understanding and prediction of pile behavior.

Declaration by Authors

Acknowledgement: None

Source of Funding: None

Conflict of Interest: The authors declare no conflict of interest.

VII. - REFERENCES

1. Abchir Z. and Burlon S. (2016) - *Contribution à l'étude du comportement des pieux soumis à des sollicitations axiales monotones et cycliques* - PhD thesis - Université Paris-Est - 286 pages.
2. Bouafia A. (2018) - *Design and calculation of geotechnical structures* - Pages Bleues Internationales.
3. Bustamante M., Frank R., Christoulas S. (1991), *Évaluation de quelques méthodes de calcul des pieux forés*. Rev. Franç. Géotech, n° 54, pp. 39-52, January 1991.
4. Bustamante M., Frank R., Gianeselli L. (1989), *Load curve prediction for isolated deep foundations*. Proceedings 12e Cong. Int. Méca. Sols et Tr. Fond, Rio de Janeiro, vol. 2, 15/6, pp. 1125-1126.
5. Cassan M. (1978), *Les essais in situ en mécanique des sols 1 Réalisation et interprétation*, Eyrolles, Paris.
6. Combarieu O. (1988) - *Amélioration des sols par inclusions rigides verticales*. Application à l'édification des remblais sur sols médiocres. *Revue française de géotechnique* n° 44.
7. Coyle H.M & Reese L.C (1966). *Load transfer for axially loaded piles in clays*. Journal of soils Mechanics and Foundations Division, ASCE, 92 (SM2) : 1-26.
8. Fleming W. G. K. (1992) - *Limit states and partial factors in foundation desing*. Proc. Instn Civ. Engrs Civ. Engng 92, 185 - 192.
9. Frank, R., Zhao, S. R. (1982). *Estimation by pressiometric parameters of settlement under axial load of bored piles in fine soils*. Bulletin de Liaison du Laboratoire des Ponts et Chaussées, 119 : 17-24.
10. Hirayama H. (1990). *Load-settlement analysis for bored piles using hyperbolic transfer function*. Soils and foundation, Vol. 30, N°1, pp.55-64.
11. Krasinski A. (2012). *Proposal for calculating the bearing capacity of screw displacement piles in non-cohesive soils based on CPT results*. Studia geotechnica et Mechanica 34 (4).
12. Maleki K. (1995). *Contribution à l'étude du comportement des micropieux isolés et en groupe*. Doctoral thesis, Ecole Nationale des Ponts et Chaussées, Paris, France.
13. Monnet J. (2007). *Numerical validation of an elastoplastic formulation of the conventional limit pressure measured with the pressuremeter Test in cohesive Soil*, ASCE, Journal of Geotechnical and Geoenvironmental Engineering, American Society of Civil Engineers, 133(9) 1119-1127.
14. Monnet J. (2013), *Mechanical characterization of the soil from the pressuremeter test*. Proceedings of the 18th International Conference on Soil Mechanics and Geotechnical Engineering, Paris, France.
15. Poulos H.G., Davis E. H. (1980) Pile foundation analysis and design. John Wiley and Sons, New York, N.Y.
16. Randolph M. F., Wroth C. P. (1978), *Analysis of deformation of vertically loaded piles*. Journal of the Geotechnical Engineering Division, December 1978, pp. 1465-1488.
17. Verbrugge J. C. (1981), *Évaluation du tassement des pieux à partir de l'essai de pénétration statique*. Revue Française de Géotechnique, n° 15, pp. 25-34.
18. Vijayvergiya V. N. (1977). *Load movement characteristics of piles*. Proceedings of Ports '77: the 4th annual symposium of the

Waterway, Port, Coastal and Ocean Division of ASCE, ASCE, New York, NY, USA, 269-284.

19. Wang Z., Xie X. and Wang J. (2012). *A new nonlinear method for vertical settlement prediction of a single pile and pile groups in layered soils*.

How to cite this article: Cheikh Ibrahima Tine, Oustasse Abdoulaye Sall, Déthié SARR. Study of the behaviour of a pile under axial load by comparative analysis of different models of the *t-z* and *q-z* load transfer curve method. *International Journal of Research and Review*. 2024; 11(9): 19-34. DOI: *https://doi.org/10.52403/ijrr.20240903*

******